Brazilian Journal of Probability and Statistics
2021, Vol. 35, No. 1, 101–118
https://doi.org/10.1214/20-BJPS497

The snap, crackle and pop of solar flares explained

Wayne S. Kendal
University of Ottawa

In memoriam: Prof. Bent Jørgensen (1954–2015), who contributed the fundamentals on which this study was based.

Abstract. The irregular fluctuations of solar flare emissions, as determined from terrestrial neutron monitors, remains poorly understood. These records empirically revealed a temporally-related variance to mean power law, $1/f$ noise and a non-Gaussian distribution, all features indicative of self-organized criticality, a theory of how derministic dynamical systems can spontaneously evolve to unstable states that express erratic changes. The non-Gaussian distribution found here approximated a Tweedie compound Poisson exponential dispersion model, a statistical distribution characterized by a variance to mean power law that itself can imply $1/f$ noise. Tweedie exponential dispersion models serve a primary role in statistical theory as foci for weak convergence for a wide range of random distributions, a role which supports an alternative conjecture to explain the solar flare fluctuations as being based on random processes rather than a deterministic system.

1 Introduction

The Neutron Monitor Database (NMDB) provides records of cosmic ray activity associated with solar flares from a worldwide network of monitors, Usoskin et al. (1997). These records fluctuate irregularly over time and mirror the numbers of sunspots, Takahashi (1989); they also have been reported to express flicker ($1/f$) and Brownian ($1/f^2$) noise, Garcia Canal, Hojvat and Taritina (2012). The mechanisms that shape these fluctuations, though, remain unclear. $1/f$ noise is conventionally explained by Self-Organized Criticality (SOC), a theory where complex and deterministic dynamical systems are postulated to naturally evolve to express $1/f$ noise, Bak and Chen (1991).

The JUNG1 monitor of NMDB is shown here to yield data that approximated a $1/f^{1.8}$ (Brownian) spectrum, it was also accompanied by irregular peaks and troughs similar to those found with multifractals. Wavelet analysis was used to confirm multifractality within these data. The normed data also approximated a Tweedie compound Poisson exponential dispersion model (EDM), Jørgensen (1997), a statistical model characterized by a variance to mean power law that implied a component of $1/f^{0.9}$ (flicker) noise within these data.

In what follows, a mathematical background will be provided to introduce self-similar stochastic processes, Tweedie EDMs, the related geometric Tweedie models, as well as wavelet analysis. This theory was applied in an exploratory analysis of the solar neutron data. On the basis of this analysis an explanation for the origin of $1/f$ noise and multifractality within these solar data was conjectured, based on the mathematical convergence effects of random data. These convergence effects, being related to the central limit theorem of statistics, provided a stochastic explanation for $1/f$ noise that was distinct from the conventional explanation for SOC, which has been predicated on the behavior of derministic dynamical systems.

Key words and phrases. Solar cosmic rays, emergent property, Taylor's power law, multifractals, weak convergence.
Received June 2019; accepted November 2020.

2 Mathematical background

2.1 Self-similar stochastic processes

This subsection follows the definitions of Leland et al. (1994), and Tsybakov and Georganas (1997): Consider the numerical sequence $Y = (Y_i : i = 0, 1, 2, \ldots, N)$, its sample mean $\hat{\mu} = \mathrm{E}[Y_i]$, deviations $y_i = Y_i - \hat{\mu}$, variance

$$\mathrm{var}[Y] = \mathrm{var}[y] = \hat{\sigma}^2 = \mathrm{E}[y_i^2],$$

and autocorrelation function

$$r(k) = \mathrm{E}[y_i\, y_{i+k}]/\mathrm{E}[y_i^2]$$

(as described for the lag k). We follow the conventional definition for self-similar stochastic processes, which characterizes these processes by virtue of their long-range correlations

$$r(k) \sim k^{-\beta} L(k), \quad k \to \infty,$$

where β is a real-valued, dimensionless, exponent bounded by $0 < \beta < 1$. The function $L(k)$ is assumed to vary slowly over large values of k.

Provided a set of non-overlapping enumerative bins of size m, one can construct a set of reproductive sequences $Y^{(m)}$ using expanding enumerative bins such that

$$Y_i^{(m)} = \frac{1}{m}(Y_{im-m+1} + \cdots + Y_{im}), \quad i > 1.$$

The integer value m is selected to keep N/m, itself, integer-valued. The mean $\hat{\mu}$ and variance $\hat{\sigma}^2$ of the primary sequence Y can be considered here as being essentially constants. The variance of $Y^{(m)}$ then would behave as a power law function of the bin size,

$$\mathrm{var}[Y^{(m)}] = \hat{\sigma}^2 m^{-\beta}, \tag{2.1}$$

if and only if the correlation of the primary sequence has the form, Tsybakov and Georganas (1997),

$$r(k) = \frac{1}{2}[(k+1)^{2-\beta} - 2k^{2-\beta} + (k-1)^{2-\beta}]. \tag{2.2}$$

We find that the limit

$$\lim_{k\to\infty} \frac{r(k)}{k^{-\beta}} = \frac{1}{2}(2-\beta)(1-\beta).$$

The correlation exponent β is related to the Hurst parameter H, where H is real-valued and confined to the interval $(0, 1)$, Mandelbrot and van Ness (1968),

$$\beta = 2(1 - H).$$

A Hurst parameter within the range $1/2 < H < 1$ indicates correlation; $H = 1/2$, Brownian motion; and $0 < H < 1/2$, anti-correlation. H also relates to the fractal dimension D, Gneiting and Schlather (2004),

$$D = 2 - H. \tag{2.3}$$

The range $1/2 < H < 1$ corresponds to $0 < \beta < 1$, the bounds for self-similar stochastic processes.

A set of additive sequences $Z^{(m)}$ can be specified on the basis of expanding enumerative bins,

$$Z_i^{(m)} = Y_{im-m+1} + \cdots + Y_{im}. \tag{2.4}$$

The reproductive and additive sequences correspond to each other by $Z_i^{(m)} = mY_i^{(m)}$; their sample means and variances similarly correspond by $\mathrm{E}[Z^{(m)}] = m\mathrm{E}[Y^{(m)}]$; and $\mathrm{var}[Z^{(m)}] = m^2\,\mathrm{var}[Y^{(m)}]$. Additive sequences, derived from Eq. (2.4), obey a variance to mean power law,

$$\mathrm{var}\big[Z_i^{(m)}\big] = m^2\,\mathrm{var}\big[Y^{(m)}\big] = \big(\hat{\sigma}^2/\hat{\mu}^{2-\beta}\big)\mathrm{E}\big[Z_i^{(m)}\big]^{2-\beta}.$$

We follow Jørgensen (1997) to designate this power law exponent by the letter p,

$$p = 2 - \beta,$$

and then,

$$H = p/2. \tag{2.5}$$

From Eqs. (2.3) and (2.5), we also have

$$p = 4 - 2D.$$

The inequality $1 < p < 2$ expresses the range of p within self-similar stochastic processes.

The biconditional relationship between Eqs. (2.1) and (2.2) implies that self-similar stochastic sequences, which express the variance to mean power law (by means of expanding bins), will express correlation functions that approximate

$$r(k) \sim c_1 k^{-\beta},$$

where c_1 is a constant.

A biconditional relationship between Eq. (2.1) and the spectral density $S(f)$ can also be derived by Fourier analysis, Tsybakov and Georganas (1997),

$$S(f) = c_2\big|e^{2\pi i f} - 1\big|^2 \sum_{l=-\infty}^{\infty} 1/|f+l|^{3-\beta}, \quad -1/2 \le f \le 1/2,$$

where the normalization constant c_2 is given by $\int_{-1/2}^{1/2} S(f)\,df = \hat{\sigma}^2$. This spectral density exhibits a singularity at $f = 0$ that approximates,

$$S(f) \sim c_3 f^{\beta-1},$$

where c_3 is a constant. The spectral density $S(f)$ also can be related to the correlation function by Fourier transformation $S(f) = \int_{-\infty}^{\infty} r(k)e^{-2\pi i f k}\,dk$, through the Wiener–Khintchine theorem, McQuarrie (1976). Spectral densities of the form $S(f) \propto f^{\beta-1}$, where $-1 < \beta < 1$, are considered to represent $1/f$ noise.

2.2 The Tweedie exponential dispersion models

In this subsection, the notation and definitions of Jørgensen (1997) will be followed. EDMs are based on the natural exponential family of distributions used to describe the error distributions of generalized linear models. We describe the distribution corresponding to the additive random variable Z, defined on the measureable set A, by

$$P_{\lambda,\theta}(Z \in A) = \int_A \exp\big[z\theta - \lambda\kappa(\theta)\big]\nu_\lambda(dz);$$

ν_λ represents the interrelated measures; θ the canonical parameter; λ the index parameter; $\kappa(\theta) = 1/\lambda \log \int e^{\theta z}\nu_\lambda(dz)$ the cumulant function and z the canonical statistic. The cumulant generating function (CGF) for the additive EDMs ED*(θ, λ) is

$$K^*(s;\theta,\lambda) \equiv \log \mathrm{E}\big(e^{sz}\big) = \lambda\big[\kappa(\theta+s) - \kappa(\theta)\big],$$

with s being the generating function variable. The function $\tau(\theta) = \kappa'(\theta)$ is the mean value mapping that can be used to define the variance function $V(\mu) \equiv \tau'[\tau^{-1}(\mu)]$ as a function of the mean value parameter μ. Note that $\tau^{-1}(\mu)$ indicates the inverse function, not the reciprocal.

$P_{\lambda,\theta}$, specified for the range of θ, represents the family $\mathrm{ED}^*(\theta, \lambda)$ that is completely determined by θ, λ and $\kappa(\theta)$. For the n independent additive random variables $Z_i \sim \mathrm{ED}^*(\theta, \lambda_i)$ with fixed θ and various values of λ we can specify that the distribution of the sum $Z_+ = Z_1 + \cdots + Z_n$ belongs to the family with the same θ, $Z_+ \sim \mathrm{ED}^*(\theta, \lambda_1 + \cdots + \lambda_n)$. This property is called closure under additive convolution.

We designate the family of reproductive EDMs by $\mathrm{ED}(\mu, \sigma^2)$, specified with the mean value and dispersion parameters μ and σ, and where $\sigma^2 = 1/\lambda$. We can further specify that the n independent reproductive random variables $Y_i \sim \mathrm{ED}(\mu, \sigma^2/w_i)$ with weighting factors w_i, summed $w = \sum_{i=1}^n w_i$, under weighted averaging gives $1/w \sum_{i=1}^n w_i Y_i \sim \mathrm{ED}(\mu, \sigma^2/w)$. The weighted averaging of independent variables with fixed μ and σ^2, as well as various values of w_i, thus belongs to the family of EDMs with the same μ and σ^2. This property is called closure under reproductive convolution.

A third property that EDMs may possess is scale invariance. In such cases the reproductive EDMs $\mathrm{ED}(\mu, \sigma^2)$ obeys the transformation rule, Jørgensen (1997),

$$c \cdot \mathrm{ED}\big(\mu, \sigma^2\big) = \mathrm{ED}\big(c\mu, c^{2-p}\sigma^2\big),$$

where c is a positive constant and p is a real-valued and unitless constant. With closure under these scale transformations the transformed random variable $\hat{Y} = cY$ will belong to the same family of EDMs with fixed μ and σ^2 but different values of c. The variance function correspondingly is transformed $V(c\mu) = g(c)V(\mu)$. This scale invariance then implies that $g(c) = V(c)$, and so $V(\mu) = \mu^p$, Jørgensen (1997).

The Tweedie EDMs are a subclass of EDMs characterized by the properties of closure under additive and reproductive convolution as well as under scale transformation. They are further subclassified into the additive $\mathrm{Tw}_p^*(\theta, \lambda)$ and reproductive $\mathrm{Tw}_p(\mu, \sigma^2)$ Tweedie EDMs. The additive random variables $Z \sim \mathrm{Tw}_p^*(\theta, \lambda)$ are related to the reproductive random variables $Y \sim \mathrm{Tw}_p(\mu, \sigma^2)$ by the duality transformation, $Y \mapsto Z = Y/\sigma^2$. The additive Tweedie variables have the population variance $\mathrm{Var}(Z) = \lambda V(\mu)$ and mean $\mathrm{E}(Z) = \lambda\mu$, and obey the variance to mean power law

$$\mathrm{Var}(Z) = a\mathrm{E}(Z)^p,$$

where $a = \lambda^{1/(\alpha-1)}$. We introduce the dimensional exponent α, which relates to the power law exponent p by

$$\alpha = (p-2)/(p-1),$$
$$p = (\alpha-2)/(\alpha-1).$$

Given Eq. (2.4), α also relates to the fractal dimension D by

$$\alpha = (2D-2)/(2D-3). \tag{2.6}$$

The interval for α that corresponds to self-similar stochastic processes is thus $(-\infty, 0)$. Parenthetically, the domain for α is $(-\infty, 1) \cup (1, \infty)$, and for θ it is $\mathbf{R}$. Note also that given the limiting case $\alpha = -\infty$, there exists a one-to-one correspondence between α and p.

Additive Tweedie EDMs have CGFs determined by the exponent p, Jørgensen (1997),

$$K_p^*(s; \theta, \lambda) = \begin{cases} \lambda e^{\theta}\big(e^s - 1\big) & p = 1, \\ \lambda\kappa_p(\theta)\big\{(1 + s/\theta)^{\alpha} - 1\big\} & p \neq 1, 2, \\ -\lambda \log(1 + s/\theta) & p = 2. \end{cases} \tag{2.7}$$

The cumulant function $\kappa_p(\theta)$ for the Tweedie EDMs is given by Jørgensen (1997),

$$\kappa_p(\theta) = \begin{cases} e^{\theta} & p = 1, \\ \dfrac{\alpha - 1}{\alpha}\left(\dfrac{\theta}{\alpha - 1}\right)^{\alpha} & p \neq 1, 2, \\ -\log(-\theta) & p = 2. \end{cases}$$

The Tweedie EDMs are classified by their exponents p, and include the extreme stable distribution ($p < 0$), Gaussian distribution ($p = 0$), Poisson distribution ($p = 1$), gamma distribution ($p = 2$), positive stable distributions ($2 < p < 3$ and $p > 3$), inverse Gaussian distribution ($p = 3$), as well as the Tweedie compound Poisson distribution for which $1 < p < 2$, Jørgensen (1997). By virtue of the range of p associated with self-similar stochastic processes, the Tweedie compound Poisson distribution could be considered as a candidate distribution to model these processes.

The middle CGF in Eq. (2.7) indicates that the compound Poisson distribution represents a summation of a random (Poisson distributed) number of independent and identically distributed (i.i.d.) gamma distributed variables. It is applied to positive valued sequences, only. In terms of its representation of solar neutron data these would correspond to the sum of a Poisson-distributed number of gamma-distributed bursts; the value $-\alpha$ would specify the (fractional) number of exponential distributions convolved together to construct the gamma distribution. This exponent α from Eq. (2.7) is also related to the shape parameter of the gamma distribution.

The additive compound Poisson probability density

$$p^*(z; \theta, \lambda, \alpha) = c^*(z; \lambda) \exp\bigl[\theta \cdot z - \lambda\kappa(\theta)\bigr] \tag{2.8}$$

does not exist in closed form but can be specified by the equations, Jørgensen (1997),

$$c^*(z; \lambda) = \begin{cases} \dfrac{1}{z} \displaystyle\sum_{n=1}^{\infty} \lambda^n \kappa^n (-1/z) / \Gamma(-\alpha \cdot n) n! & \text{for } z > 0, \\ 1 & \text{for } z = 0. \end{cases}$$

The parameter $-\alpha$ assumes a positive non-integer value that is related to the fractal dimension D. Inversion of Eq. (2.6) gives

$$D = (3\alpha - 2)/\bigl[2(\alpha - 1)\bigr].$$

We also have,

$$D = 2 - p/2.$$

The fractal dimensions associated with self-similar stochastic processes is therefore $1 < D < 1.5$.

The Tweedie EDMs have a fundamental role in statistical theory as foci of convergence for a broad range of distribution functions, similar to the role that the Gaussian distribution has in the central limit theorem, Jørgensen (1997). This convergence theorem is primarily directed towards the variance function of the EDMs whereas in the central limit theorem the focus is towards the Gaussian distribution itself.

Jørgensen, Martínez and Tsao (1994) have proven that for EDMs $\mathrm{ED}(\mu, \sigma^2)$ with variance functions that approximate $V(\mu) \sim \mu^p$ as either $\mu \to 0$ or $\mu \to \infty$ then $c^{-1}\,\mathrm{ED}(c\mu, \sigma^2 c^{2-p})$ will converge towards a Tweedie EDMs as $c \downarrow 0$ or $c \to \infty$. Indeed the variance functions of many EDMs will approximate $V(\mu) \propto \mu^p$ as $\mu \to 0$ or $\mu \to \infty$. Since EDMs can be used to represent a broad range of probability distributions this theorem has a similarly broad range of application. It relates to stable generalizations of the central limit theorem, and

consequently the Tweedie EDMs can be considered to have a role analogous to the Gaussian distribution, Jørgensen (1997). For the particular cases where $p = 0$ and $p = 1$ this Tweedie convergence theorem has as its focus the Gaussian and Poisson distributions, suggesting that the convergence theorem acts to unify the central limit and Poisson convergence theorems, Jørgensen (1997).

2.3 The geometric Tweedie models

A second family of Tweedie models exists called the geometric Tweedie models, which govern geometric sums of random variables. Jørgensen and Kokonendji (2011) have described the theory for geometric Tweedie models in detail; this section will provide only a brief introduction.

We define the geometric sum $S(\bar{q})$ is on the probability parameter $\bar{q} \in (0, 1]$ for the i.i.d. random variables $X_1, X_2, \ldots$, independent of the geometric random variable $N(\bar{q})$,

$$S(\bar{q}) = \sum_{k=1}^{N(\bar{q})} X_k.$$

$N(\bar{q})$ has a probability mass function $\Pr[N(\bar{q}) = k] = \bar{q}(1-\bar{q})^{k-1}$ for $k = 1, 2, \ldots$ with $N(1) \equiv 1$. If the CGF for X is defined as $K(s) = K(s; X) = \log \mathrm{E}(e^{sX})$ the geometric cumulant function (GCF) is,

$$C(s) = C(s; X) = 1 - e^{-K(s)} \quad \text{for } s \in \bar{D}(C),$$

with a domain $\bar{D}(C) = \{s \in \mathbf{R} : C(s) < 1\} = \mathrm{dom}(K)$.

The geometric random variable $N(\bar{q})$ has the moment generating function (MGF)

$$\mathrm{E}\big[e^{sN(\bar{q})}\big] = \big[1 - \bar{q}^{-1}\big(1 - e^{-s}\big)\big]^{-1} \quad \text{for } s < -\log(1-\bar{q}).$$

Its GCF is

$$C\big(s; N(\bar{q})\big) = \bar{q}^{-1}\big(1 - e^{-s}\big) \quad \text{for } s < -\log(1-\bar{q}).$$

The geometric sum has the MGF, Jørgensen (1997, Jørgensen and Kokonendji (2011)

$$\mathrm{E}\big[e^{sS(\bar{q})}\big] = \mathrm{E}\big[e^{N(\bar{q})K(s)}\big] = \big\{1 - \bar{q}^{-1}\big[1 - e^{-K(s)}\big]\big\}^{-1} = \big[1 - \bar{q}^{-1}C(s)\big]^{-1} \quad \text{for } s \in D\big(\bar{q}^{-1}C\big).$$

The GCF of the geometric sum $S(\bar{q})$ is further represented by $C(s; S(\bar{q})) = \bar{q}^{-1}C(s)$ for $s \in \bar{D}(\bar{q}^{-1}C)$.

The additive geometric dispersion models $\mathrm{GD}^*(\mu, \hat{\gamma})$ are closed under geometric compounding. For a sequence of i.i.d. random variables $\{X_k\}$ with distribution $\mathrm{GD}^*(\mu, \hat{\gamma})$, their geometric sum will be distributed in accord with

$$\sum_{k=1}^{N(\bar{q})} X_k \sim \mathrm{GD}^*(\mu, \hat{\gamma}\bar{q}) \quad \text{for } \bar{q} \in (0, 1].$$

Jørgensen and Kokonendji (2011) defined the v-function, in analogy to the variance function $V(\mu)$ introduced earlier. The family of geometric Tweedie models $\mathrm{GD}(\mu, \hat{\gamma})$, with mean μ and dispersion parameter $\hat{\gamma}$, is thus characterized by a power law v-function $v(\mu) = \lambda\mu^p$, where the constant $\lambda > 0$. These models obey the scaling rule

$$c^{-1}\,\mathrm{GD}\big(c\mu, c^{2-p}\hat{\gamma}\big) = \mathrm{GD}(\mu, \hat{\gamma}).$$

Geometric dispersion models with v-functions asymptotic to $v(\mu) = \mu^p$ are required to converge towards the geometric Tweedie models as their domains of attraction, Jørgensen and Kokonendji (2011).

The geometric Tweedie dispersion models are similarly categorized by their power law exponent p. They include the geometric extreme stable models, $p < 0$; the asymmetric Laplace model, $p = 0$; the geometric Poisson model, $p = 1$; the geometric compound Poisson model, $1 < p < 2$; the geometric gamma model, $p = 2$; the geometric Mittag-Leffler models, $p > 2$; and models with exponential v-functions, $p = \infty$. The asymmetric Laplace model can be represented by the probability density function,

$$f(x;\hat{\mu},\hat{\gamma},\hat{m}) = \frac{1}{\sqrt{2\hat{\gamma}+\hat{\mu}^2}} \exp\left\{\frac{1}{\hat{\gamma}}\left[(x-\hat{m})\hat{\mu} - |x-\hat{m}|\sqrt{2\hat{\gamma}+\hat{\mu}^2}\right]\right\},$$

where $\hat{m}$ is its mode, and $\hat{\mu}$ and $\hat{\gamma}$ are its mean and variance respectively, Jørgensen and Kokonendji (2011). Note that, because of its value $p = 0$, this distribution is analogous to the Gaussian distribution, where as a Tweedie EDM it also assumes the value $p = 0$.

2.4 Wavelet analysis

Self-similar stochastic processes may demonstrate local variations in the fractal dimension along their sequence. Wavelet analysis may be used to construct a singularity spectrum from such data, Muzy, Bacry and Arnedo (1993b), Goldberger et al. (2000). A wavelet transform $T_\psi[f](\tilde{b},\tilde{a})$ of a function f is typically constructed by decomposition into contributions from an analyzing wavelet ψ by means of translations and dilations specified through the real-valued scale and shape parameters $\tilde{a} \in \mathbf{R}^+$ and $\tilde{b} \in \mathbf{R}$,

$$T_\psi[f](b,a) = \frac{1}{\tilde{a}} \int_{-\infty}^{+\infty} \psi\left(\frac{x-\tilde{b}}{\tilde{a}}\right) f(x)\,dx.$$

Wavelets may be formed from repeated derivatives of the Gaussian function,

$$\psi^{(N)}(x) = d^N\left(\mathrm{e}^{-x^2/2}\right)/dx^N.$$

The local Hölder exponent $h(x_0)$ is then used to characterize singularities of a function f at specified point x_0, and represents the largest exponent for which a polynomial $P_n(x)$ of order n exists to satisfy the relation,

$$\left|f(x) - P_n(x-x_0)\right| = O\left(|x-x_0|^h\right),$$

in some neighborhood of x_0.

From this analysis a $D(h)$ singularity spectrum can be constructed to represent the Hausdorff dimension for which the Hölder exponent attains the value h, Muzy, Bacry and Arnedo (1993a),

$$D(h) = \dim_H\left[x \mid h(x) = h\right].$$

This analysis is essentially qualitative: For monofractal data $D(h)$ would yield only a single point; for multifractal data $D(h)$ would yield an inverted curve.

2.5 Self-organized criticality and $1/f$ noise

$1/f$ noise has been loosely defined to include frequency spectra of the form $S(f) \propto 1/f^{1-\beta}$, with $0 < 1-\beta < 2$; more stringently, it is defined with $0.5 < 1-\beta < 1.5$, Press (1978). These definitions overlap the range $0 < 1-\beta < 1$ for self-similar stochastic processes and the compound Poisson EDM. Traditionally, $1/f$ (pink) noise has been considered to be bounded by white noise $1-\beta = 0$ and Brownian (random walk) noise $1-\beta = 2$.

$1/f$ noise has been reported from a wide variety of physical and biological processes, including electrical currents, oceanic currents, sea levels, the intensity and pitch of music,

the luminosity of stars, Press (1978), fluctuations in neuronal activity, blood pressure, heart rate, and electroencephalogram measurements, Musha and Yamamoto (1997). In fact, some authorities have labeled $1/f$ noise as being ubiquitous, Bak, Tang and Wiesenfeld (1987). Many explanations for $1/f$ noise have been proposed, Dutta and Horn (1981) and Szendro, Vincze and Szasz (2001); the most notable of these explanations being SOC, Bak, Tang and Wiesenfeld (1987).

SOC is a hypothesis, based on the behavior of deterministic dynamical systems. Dynamical systems, in mathematical terms, consist of coupled first order ordinary differential equations, Abraham (1996); in physical terms these systems are focused on physical situations like those described by Hamilton's equations of motion, Susskind and Hrabovsky (2013). Such systems yield deterministic trajectories in phase space. There is, however, also a class of stochastic dynamical systems for which both the trajectory of the process and the initial conditions are not predictable, Eubank and Farmer (1996).

Bak, Tang and Wiesenfeld (1988) postulated $1/f$ noise as being a deterministic response of the system to what they termed the self-organized critical state. In this hypothesis, dynamical systems with multiple degrees of freedom were postulated to assume unstable states that could express $1/f$ noise, without the necessity of adjustments from external influences. This description of SOC was semi-quantitative, and it was supported by simulations devised to represent the growth and collapse of sandpiles that yielded $1/f$ noise, Bak, Tang and Wiesenfeld (1988).

SOC is identified empirically in natural processes through the demonstration of long-range correlations and $1/f$ noise associated with a non-Gaussian distribution, Nurujjaman and Sekar Iyengar (2007). To this date no complete mathematical description for SOC has found general acceptance, although the dynamical mean-field model has been considered promising in this accord, Vespignani and Zapperi (1998).

The dynamical systems postulated within SOC are called organized for reason of the long-range correlations that have been interpreted as non-random effects, Frigg (2003). Similarly the variance to mean power law, by virtue of its over-dispersed clustering, has also been interpreted as a non-random effect, and could be considered to represent an emergent effect of self-organization.

These dynamical systems are termed critical on the basis of unpredictable changes that can be precipitated by a single local event, Frigg (2003), and by analogy to critical point effects associated with phase transitions, Bak, Tang and Wiesenfeld (1987). This criticality appears to manifest spontaneously without apparent external influence, justifying the claim of self-organization, Frigg (2003).

Central to this hypothesis is the analogy to phase transitions in equilibrium statistical mechanics, Bak, Tang and Wiesenfeld (1988). Similar transitions have been found to occur within the Ising model of ferromagnetism, Pathria (1972). Shan et al. (2014), in a related analysis of quantum phase transitions, identified sharp peaks in the derivative of a quantity they referred to as geometric quantum discord; this occurred close to a critical point for a phase transition. The sharp peak, itself, was used to substantiate the presence of critical changes in their dynamical system. Such critical points are central to the concept of SOC.

One additional feature of SOC warrants mention: Bak, Tang and Wiesenfeld (1988) claimed that at the site of these critical points "spatial self-similarity can occur, and that the dynamical response functions at those sites manifest a characteristic power-law, $1/f$ noise, behavior". These frequency spectra obey the equation $S(f) \propto 1/f^{1-\beta}$ with $1-\beta$ being "only roughly equal to 1.0", and thereby indicating a fractal (self-similar) structure. For the exponent $1-\beta$ to fall within the same range as for the Tweedie compound Poisson EDM and self-similar stochastic processes we could anticipate the fractal dimensions to range $1 < D < 1.5$.

3 Data analysis

Neutron data were available from NMDB (http://www.nmdb.eu/nest/search.php) and their consortium of monitoring sites: AATB, APTY, ARNM, ATHN, CALM, DJON, DRBS, HRMS, INVK, JUNG, JUNG1, KERG, KIEL, LMKS, MCRL, MOSC, MXCO, NAIN, NAMN, NEWK, OULU, PSNM, THUL, and TIBT. Sunspot data were provided by the World Data Center for the Sunspot Index and the Royal Observatory of Belgium (http://sidc.be/silso/datafiles). Daily records for the JUNG1 neutron monitor MN64 from Jan. 1, 1988 to Dec. 31, 2017) were plotted (Figure 1a, bottom line) and compared to the corresponding sunspot counts (top line). The neutron counts correlated negatively with the sunspot cycle ($r = -0.679$, 95% CI -0.689 to -0.669, $N = 10{,}925$). They also exhibited irregular peaks and troughs that were repeated over multiple measurement scales, a feature suggestive of fractals and multifractals, Stanley and Meakin (1988).

The JUNG1 data were resolved into sinusoidal components by Fourier analysis, and an intensity spectrum of these components was plotted against the respective frequencies (Figure 1b). In order for the discrete Fourier transform (DFT) to be applied, the mean had to be subtracted from these data, the data detrended, and the sequence padded with zeros at its end to raise the number of data points to next largest power of 2 ($N_{\text{packed}} = 16{,}384$). A Hamming window 5 data points long was applied to smooth the spectrum from additional random effects and the DFT calculated. A power spectrum was constructed by multiplying the transformed data sequence with its complex conjugate. Linear regression was conducted between the logarithms of the spectral density and frequency over a region of apparent linearity to yield a $1/f^{1.8}$ spectrum.

Whereas the exponent came within the broader range for $1/f$ noise, it was close to that of $1/f^2$ (Brownian) noise. The overall spectrum had a flat region on its left side, attributable to

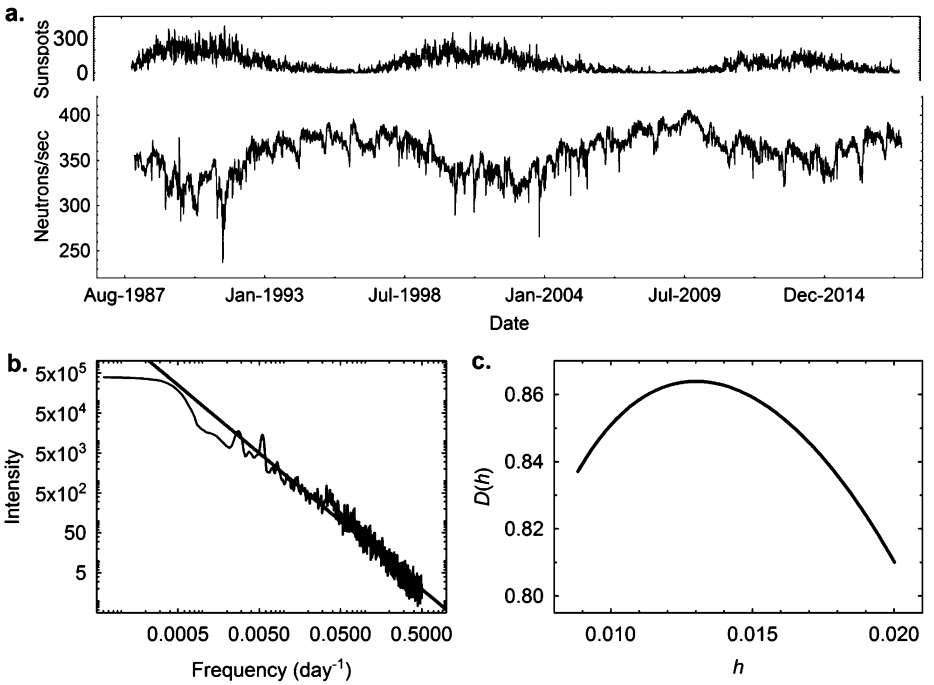

Figure 1 *a. Sequential counts from the JUNG*1 *neutron monitor* (*bottom line*) *and daily sunspot counts* (*top line*). *b. Frequency spectrum for JUNG*1 *fluctuations. A frequency spectrum was constructed to provide the intensity of neutron count fluctuations as a function of frequency. The log–log plot revealed an approximately linear pattern* (*solid line inserted for comparison*). *c. Singularity spectrum of the JUNG*1 *fluctuations.*

the finite size of the data set and the packing with zeros. This was interpreted as an artifact of the discrete Fourier transform.

The maximal peak of the frequency spectrum occurred at about 2×10^{-4} days^{-1}, which corresponded to the 11-year sunspot cycle. A superimposed straight line represented a hypothetical $1/f^{1.8}$ spectrum, and was derived by linear regression of a portion of these data that had been selected subjectively. Additional regression parameters such as the standard error and 95% CI were not calculated for reason that the packing with zeros would have biased such estimates and because of the subjectivity associated with choice of the data points for regression.

There was a slight inflection in the middle of this portion of the spectrum. Other investigators, from a different analysis of the Auger observatory data, reported a similar inflection they attributed to a mixture of $1/f$ and $1/f^2$ noise, Garcia Canal, Hojvat and Taritina (2012). In the present analysis for reason of the inflated value for N_{packed}, the apparent finite size effects, the subjective choice of data for regression, and the use of the Hamming window to smooth the data, statistical comparison of regression parameters between different regions of the linear spectrum was not deemed practical.

Wavelet analysis was conducted next in order to resolve the JUNG1 data into wavelet components, Goldberger et al. (2000). These were used to construct a singularity spectrum $D(h)$ by plotting the fractal (Hausdorff) dimension D against a scaling (Hölder) exponent h (Figure 1c), Muzy, Bacry and Arnedo (1993b). Monofractal data treated this way would typically be represented by a single point; multifractal data by an inverted curve that reflected a range of fractal dimensions. The JUNG1 data revealed an inverted curve indicative of multifractality. A qualitative demonstration of an inverted $D(h)$ curve was considered to be the endpoint of this analysis; in conventional practice there would be no role for statistical inferences to be derived from the $D(h)$ curve.

The analysis then shifted to a time domain study of the JUNG1 data, in order to better determine whether or not $1/f$ noise might be detectable within the detrended data of Figure 1a, Tsybakov and Georganas (1997). The absolute values of the detrended data were divided into a sequence of equal-sized and non-overlapping enumerative bins; data within each bin were summed; and the sample mean μ and sample variance σ^2 of these sums were estimated. These calculations were repeated for expanding enumerative bins, Eq. (2.4), and the resultant means and variances plotted against each other on a log–log scale (Figure 2a).

Figure 2a indicated a linear relationship. An underlying power law $\sigma^2 \propto \mu^p$ was evident, with the exponent $p = 1.9$, derived by linear regression. Since the variance and mean assessments were obtained from expanding enumerative bins that reused data, additional regression assessments like the standard error and 95% confidence interval for the slope would have been biased and thus were not calculated.

The method of expanding enumerative bins, though, was employed because this method leads to a biconditional relationship between $1/f^{1-\beta}$ noise and the variance to mean power law (Eqs. (2.1) and (2.2)), Tsybakov and Georganas (1997). This method is also related to a procedure called detrended fluctuation analysis, that has been employed for similar purposes, Kantelhardt et al. (2001)). The power law exponents of the frequency spectrum and the variance to mean power law, determined from Figures 1b and 2a, can be linked by the relationship $p \sim 2 - \beta$. On this basis a component of $1/f^{0.9}$ noise could be surmised from Figure 2a.

Since the JUNG1 data yielded $p = 1.9$, the Tweedie compound Poisson distribution was selected as a candidate model to be evaluated against an empirical frequency distribution derived from these data. A candidate theoretical cumulative distribution function (CDF) was obtained by numerical integration over z in Eq. (2.8) using arbitrary initial estimates for the adjustable parameters θ, λ, and α. This theoretical CDF was iteratively fitted to an empirical

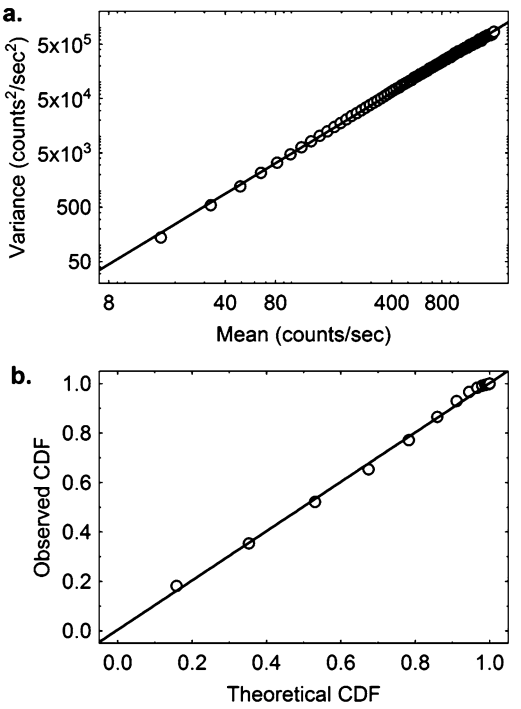

Figure 2 *a. Variance to mean power law. b. Probability-probability plot. The adjustable parameters were,* $\theta = -0.19$, $\lambda = 1.4$, *and* $p = 1.5$.

CDF derived from the normed detrended neutron data using the Levenberg–Marquardt algorithm for minimization of the summed least square differences. By this means, successively improved estimates for these parameters were obtained. A probability-probability plot on the basis of the optimized parameters was then constructed; the linear relationship indicated a qualitative agreement between the theoretical CDF and empirical CDF (Figure 2b).

This analysis served as a visual means to evaluate the proposed model. Since the choice of plotting positions in such an analysis was subjective, this probability-probability plot should not be expected to provide quantitative inferences, Bury (1999). With this caveat in mind, though, the value of p determined from the iterative fit was $p = 1.5$, consistent with both the theoretical range of p from the Tweedie compound Poisson EDM and the analysis from Figure 2a.

The exponent p from the variance to mean power law was related to the fractal dimension D of the data sequence by the equation $p = 4 - 2D$ (Section 2.1). This analysis from Figure 2a provided a global assessment of the power law exponent p from the JUNG1 data, and was not designed to demonstrate whether or not local variations might occur within the data sequence. The singularity spectrum (Figure 1c), thought, indicated that D (and consequently both α and p) should vary locally within these data.

To further investigate for local variations, the normed and detrended data from Figure 1a were divided into sequential non-overlapping segments of 100 days in length. Local values for α were then estimated for each segment using the expanding bin method from Eq. (2.4). In order to increase the sample size, data from 23 other NDMB neutron monitors were included in this analysis.

Figure 3 provided a frequency histogram derived from the combined analysis. A unimodal histogram was obtained with its mode at $\alpha = -0.15$ ($p = 1.86$), located just below the transition point $\alpha = 0$ ($p = 2$) where the compound Poisson distribution would be replaced by

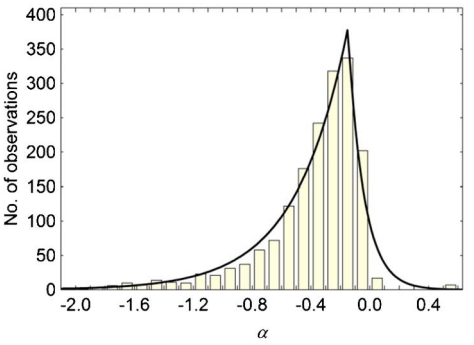

Figure 3 *Frequency histogram for local values of* α. *An asymmetrical Laplace distribution was fitted to the histogram* (*solid black line*).

the gamma distribution. The solid black line denoted the best fit of an asymmetric Laplace distribution, Kozubowski and Podgórski (2001), explored here to model the histogram.

The asymmetric Laplace distribution is a member of the family of geometric Tweedie models, which represent geometric sums of random variables and are analogous to the Tweedie EDMs mentioned earlier, Jørgensen and Kokonendji (2011). As noted above, the asymmetric Laplace distribution is the geometric random equivalent to the Gaussian distribution. The derivative of the asymmetric Laplace distribution with respect to α does not exist at its peak; hence this peak represents a mathematical critical point, which notably was located just below the transition point $\alpha = 0$.

Even with the added data from the other neutron monitors the sample size used to construct this histogram was relatively small. A chi-squared goodness of fit analysis confirmed a statistically significant difference (probability value <0.001) between the histogram and the fitted asymmetric Laplace distribution. This difference was not surprising given that the 11 year sunspot cycle as well as spurious influences in the measurements had been included in this analysis (Figure 1a). The application of the asymmetric Laplace to this histogram would have some theoretical justification given the mathematical convergence theorem that governs geometric dispersion models (Section 2.3), and the analogous role that the mathematical critical point from the asymmetric distribution has to critical points in SOC. For these reasons and for reason of the qualitative correspondence of the histogram to the asymmetric Laplace distribution, this distribution could nevertheless be considered to represent an exploratory model with which to conjecture processes that might be at play in the development of SOC and multifractality.

4 Discussion

4.1 Convergence towards a Tweedie compound Poisson distribution yields $1/f$ noise

In Section 3, the sequential measurements of solar radiation from the JUNG1 neutron observatory conformed to a variance to mean power law $\sigma^2 = a\mu^{1.9}$; for this reason a Tweedie compound Poisson EDM (which inherently expresses a variance to mean power law with exponent $1 < p < 2$) was used to describe these measurements.

The Tweedie convergence theorem (Section 2.2) showed that for EDMs with variance functions that approximate a power law for either large or small values of μ will be required to converge towards the variance functions of the Tweedie EDMs, Jørgensen (1997). Since probability distribution functions that possesses a finite CGF will belong to an EDM, and there exist many probability distributions that have variance functions approximating $V(\mu) \sim$

μ^p, a wide variety of random data would be expected to come within the domain of attraction of the Tweedie EDMs, Kendal and Jørgensen (2011).

Variance to mean power laws, mathematically identical to the power law that characterizes the Tweedie EDMs have been reported from the spatial aggregation of animal and plant species (where they are referred to as Taylor's power law), Taylor et al. (1983), the clustering of Human Immunodeficiency Virus (HIV) cases, Anderson and May (1988) and Petterle et al. (2019), regional organ blood flow, Kendal (2001), the temporal clustering of measles cases in epidemics, Keeling and Grenfell (1999), the spatial clustering of leukemia cases, Philippe (1999), and a wide range of physical and econometric processes that manifest fluctuation scaling, Eisler, Bartos and Kertesz (2008). A wide range of ad hoc population dynamic models as well as physical and mathematical models have been proposed to explain this variance to mean power law, notwithstanding the family of statistical models discovered by Tweedie (1984) and now called the Tweedie EDMs by Jørgensen (1997).

Power laws like the variance to mean power law are commonly expressed by dynamical systems that exhibit chaotic behavior. The term chaos refers to an apparently random (pseudorandom) behavior accompanied by a sensitive dependence upon initial parameters, Werndl (2009). Such chaotic behavior, even though being deterministic, may manifest a probability distribution and variance function that comes within the domain of attraction of the Tweedie EDMs.

The solar neutron data, analysed in Section 3, were shown through Fourier analysis to approximate a $1/f^{1.8}$ frequency spectrum, itself a power law. Further, time domain, analysis revealed that there was a component of $1/f^{0.9}$ noise within these data, which would fall within a more restrictive description of $1/f$ noise. We noted within Section 2.5 that there are many explanations for $1/f$ noise. One of the most popular of these explanations is SOC, where it is postulated that deterministic dynamical systems can spontaneously evolve to express chaotic (power law) behavior, particularly that of $1/f$ noise.

In Sections 2.1 and 2.2, it was mentioned that a wide variety of random and pseudorandom data may express variance to mean power laws with $1 < p < 2$. Such sequential data could potentially be described by self-similar stochastic processes as well as the Tweedie compound Poisson EDM. The solar neutron data was conjectured to have a major component that behaved this way. A biconditional relationship between the variance to mean power law and $1/f$ frequency spectra provided a mechanistic explanation for the origin of the $1/f$ noise apparent to these data, being based on the Tweedie convergence theorem, Kendal and Jørgensen (2011).

The Tweedie convergence theorem has been proven for i.i.d. random variables, Jørgensen (1997), whereas the variance to mean power law $\sigma^2 \propto \mu^{1.9}$ (Figure 2a) apparent to the solar neutron data indicated long-range correlations and $1/f^{0.9}$ noise. This finding might seem inconsistent with the specification for i.i.d. random variables in the Tweedie convergence theorem. It is conceivable, though, that this specification might be more restrictive than necessary, Kendal (2017). Consider, for example, the development of the central limit theorem: Its initial proofs required i.i.d. random variables; later proofs, though, allowed for correlated and dissimilar variables, Fischer (2011).

Section 2.5 provided a brief description of $1/f$ noise, an arguably ubiquitous noise pattern considered by some to represent deterministic behavior originating from SOC. There have been many other explanations for $1/f$ noise proposed (see, for example, Dutta and Horn (1981), Press (1978), and Musha and Yamamoto (1997)), but these have largely represented ad hoc models. Whereas SOC gives a general explanation for $1/f$ noise, it remains a qualitative hypothesis justified primarily by simulations designed, in the first place, to yield $1/f$ noise, Frigg (2003). As well, this hypothesis lacks a generally accepted mathematical description.

The exploratory analyses presented here indicated that $1/f$ noise might represent a major component of the solar flare data and that self-similar random processes as well as the Tweedie compound Poisson EDM could provide a mathematical description for this component. In this context, the origin of $1/f$ noise could be explained by the convergence behavior of random (or pseudorandom) data, as governed by the Tweedie convergence theorem, Kendal and Jørgensen (2011).

As such, it was not necessary to postulate the existence of a deterministic dynamical system to explain the origins of $1/f$ noise. The apparent correspondence of these data to the Tweedie compound Poisson distribution would indicate that solar neutron data could be modeled by a random (Poisson)-distributed number of radiative bursts that occur within a given time period, where the intensity of the bursts is distributed in accordance with a gamma distribution. The gamma distribution would be further subject to variations in its dimensional parameter α that would cause these data to have multifractal properties.

A mechanistic explanation for the origin of $1/f$ noise based on the Tweedie convergence theorem would provide a fundamental and general basis to explain this noise, similar to how the central limit theorem provides fundamental understanding of normally-distributed random processes that arise within nature. Since chaotic (pseudorandom) data may, in some situations, manifest with probability distribution functions that come within the domain of attraction of the Tweedie models, a hypothesis for the origin of $1/f$ noise based on the Tweedie convergence theorem would not necessarily exclude the role of deterministic dynamical systems in this matter.

4.2 Convergence towards an asymmetric Laplace distribution may contribute to multifractality

The solar neutron data also revealed a pattern of irregular peaks and troughs, comprised of numerous low amplitude high-frequency oscillations modified by larger amplitude low-frequency oscillations, consistent with multifractality (Figure 1a). A singularity spectrum constructed from these data yielded an inverted curve that confirmed multifractality (Figure 1c). This multifractality implied that the fractal dimension of the data sequence, and consequently the Tweedie parameters p and α, would vary over the length of the data sequence. An analysis of sequential, non-overlapping, segments from these data confirmed the presence of such variations in α throughout the sequence (Figure 3).

The resultant frequency histogram for the values of α was unimodal, with the mode placed just below the transition point where the Tweedie compound Poisson EDM ($\alpha < 0$) is replaced by another Tweedie EDM, the gamma distribution ($\alpha = 0$). Had this histogram consisted of a single point, the solar neutron data would have been monofractal; the range of values that was evident with α was instead consistent with multifractality.

Section 2.3 provided an introduction to the geometric Tweedie models, Jørgensen and Kokonendji (2011). These models describe geometric sums of random variables; they act as domains of attraction for random geometric sums. One particular geometric Tweedie model, the asymmetric Laplace distribution, was fitted to the histogram of the Tweedie dimensional parameter α (Figure 3).

The asymmetric Laplace distribution only qualitatively corresponded to the frequency histogram for values of α; there was a statistically significant difference in the fit between this distribution and the histogram. This difference could perhaps be attributed to the superimposition of the sunspot periodicity as well as random artifact. In other published studies, related analyses derived from the eigenvalue deviations of the Gaussian Unitary Ensemble (GUE), the deviations of the Chebyshev prime counting function Kendal (2014), as well as the growth fluctuations of bristlecone pine trees Kendal (2017) revealed multifractality associated with

a similar unimodal histogram for the Tweedie parameter α that similarly centered just below the transitional point $\alpha = 0$. It would be conjectured here that this resemblance is not an artifact or an accident, but rather reflects a particular behavior of certain types of random data.

Curiously, Wigner (1967) proposed that the eigenvalues of the GUE could model the energy levels of large nuclei, and Dyson and Montgomery (unpublished communication, 1972) conjectured that these eigenvalues could be linked to the Riemann hypothesis that the nontrivial zeros of the Riemann zeta function are located in the complex plane on a vertical line with real value of $1/2$, Hayes (2003). One might then conjecture that the Tweedie convergence theorems might also have a role in the distribution of the prime numbers and nuclear energy levels, Kendal (2014) and Kendal and Jørgensen (2015), as well as solar neutron fluctuations and the growth of bristlecone pine trees.

Granted the conjecture that an asymmetric Laplace distribution might describe the distribution of the Tweedie dimensional parameter α with the peak of this distribution located just below $\alpha = 0$, there would be another implication worth consideration. The peak of the Laplace distribution is non-differentiable and so represents a mathematical critical point. The associated multifractality might then be attributed to a critical balance in the distribution of the values of α.

The significance of such a critical balance is made more apparent within the hypothesis of SOC, which was based on an analogy to critical phenomena occurring with phase transitions, Bak, Tang and Wiesenfeld (1988). At the transition point between phases the dynamical variables are postulated to become unstable and manifest $1/f$ behavior. In the present study, and the cases from the literature mentioned above, the mathematical critical point of the Laplace distribution was conjectured to lie just below the transition point between adjacent Tweedie EDMs. Again, this appears not to be an artifact or an accident of nature but rather a fundamental property of certain types of random data that manifest within natural and mathematical systems.

5 Conclusion

Terrestrial neutron detectors have demonstrated a periodicity in solar neutron radiation that correlates with the 11-year sunspot cycle and is superimposed upon an irregular pattern of high-frequency fluctuations modulated by larger low-frequency fluctuations. An exploratory analysis of these solar emissions was presented here that indicated the presence of an overall $1/f^{1.8}$ noise spectrum as well as a singularity spectrum indicative of multifractality.

A conjecture was presented that these solar neutron fluctuations could be modelled by a self-similar stochastic process, more specifically by a compound Poisson Tweedie EDM, which manifested a variance to mean power law $\sigma^2 \propto \mu^{1.9}$. This power law inferred a component of $1/f^{0.9}$ noise within these fluctuations.

Similar to the role the Gaussian distribution has in statistical theory as an attractor for the central limit theorem, the variance functions of the Tweedie EDMs serve as attractors for variance functions of other random variables in a related convergence effect, Jørgensen (1997). The power law $\sigma^2 \propto \mu^{1.9}$ (and thereby $1/f^{0.9}$ noise) construed from the JUNG1 fluctuations could be attributed to Tweedie convergence.

The power law exponent $p = 1.9$ ($\alpha = -0.11$), obtained globally from the JUNG1 data, suggested that these data possessed an approximate fractal dimension of $D = 1.05$. Local analysis, though, indicated that these data were multifractal, expressing a range of values for D (as well as for p and α). This multifractality was then conjectured to be modeled by a geometric Tweedie models, the asymmetric Laplace distribution.

A second and related Tweedie convergence theorem has as its attractor these geometric Tweedie models, Jørgensen and Kokonendji (2011). It was for this reason that the asymmetric Laplace distribution was chosen as a candidate distribution to represent the histogram of α. It had a peak at $\alpha = -0.15$ indicative of a critical point attractor for the expression of this multifractality, and similar to critical points found within other natural and mathematical systems.

Much as how the central limit theorem explains why the Gaussian distribution may manifest from diverse random systems, the Tweedie convergence theorems explain how the variance to mean power law, $1/f$ noise, and multifractality can emerge within certain, scale invariant, random systems. These theorems provide a mechanistic hypothesis to explain the snaps, crackles and pops apparent within solar flare fluctuations.

Bak, Tang and Wiesenfeld (1987), however, proposed SOC as a universal explanation for the origin of $1/f$ noise; they did not include the expression of multifractality in this explanation. According to their theory, deterministic dynamical systems with multiple degrees of freedom could evolve towards unstable states that manifested $1/f$ noise; this $1/f$ noise was assumed to reflect non-random self-organization. Their hypothesis was based on an analogy to critical point effects associated with phase transitions in physics. In statistical physics these critical points are associated with strongly peaked functions representative of dynamical parameters; at such points such parameters can express power law behavior.

The Tweedie convergence theorems allow for an alternative explanation for the emergence of $1/f$ noise, multifractality, and criticality within the solar neutron data. Since these theorems were derived for random processes they might be considered inconsistent with the premise of SOC, Eubank and Farmer (1996). The distinction between random and non-random systems, however, can be ambiguous. Nonlinear systems may manifest chaotic dynamics that, although being non-random, can be practically impossible to predict (and hence appear random), Eubank and Farmer (1996). If an empirical CDF, derived from a chaotic process, can be approximated by an EDM that asymptotically yields a variance to mean power law then that EDM would be also mathematically required to converge towards one of the Tweedie EDMs, Jørgensen (1997). Hence, the Tweedie EDMs might represent such a chaotic process and SOC, Kendal (2015).

Parsimony, though, would seem to indicate that the emergence of $1/f$ noise, multifractality, and criticality within solar flare fluctuations could be more simply explained by mathematical convergence effects alone, rather than having to postulate a particular behaviour of derministic dynamical systems.

References

Abraham, R. H. (1996). Visualization techniques for cellular dynamata. In *Introduction to Nonlnear Physics* (L. Li, ed.) 296–307. New York: Springer.

Anderson, R. M. and May, R. M. (1988). Epidemiological parameters of HIV transmission. *Nature* **333**, 514–519.

Bak, P. and Chen, K. (1991). Self-organized criticality. *Scientific American* **264**, 46–53.

Bak, P., Tang, C. and Wiesenfeld, K. (1987). Self-organized criticality: An explanation of $1/f$ noise. *Physical Review Letters* **59**, 381–384.

Bak, P., Tang, C. and Wiesenfeld, K. (1988). Self-organized criticality. *Physical Review A* **38**, 364–374. MR0949160 https://doi.org/10.1103/PhysRevA.38.364

Bury, K. (1999). *Statistical Distributions in Engineering*. Cambridge: Cambridge University Press.

Dutta, P. and Horn, P. M. (1981). Low-frequency fluctuations in solids: $1/f$ noise. *Reviews of Modern Physics* **53**, 497–516.

Eisler, Z., Bartos, I. and Kertesz, J. (2008). Fluctuation scaling in complex systems: Taylor's law and beyond. *Advances in Physics* **57**, 89–142.

Eubank, S. G. and Farmer, J. D. (1996). Introduction to dynamical systems. In *Introduction to Nonlnear Physics* (L. Li, ed.) 55–105. New York: Springer. MR1431055

Fischer, H. (2011). *A History of the Central Limit Theorem: From Classical to Modern Probability Theory*. New York: Springer. MR2743162 https://doi.org/10.1007/978-0-387-87857-7

Frigg, R. (2003). Self-organized criticality—what it is and what it isn't. *Studies in History and Philosophy of Science* **34**, 613–632.

Garcia Canal, C., Hojvat, C. and Taritina, T. (2012). Scaler mode of the Auger observatory and sunspots. *The Astrophysical Journal Supplement Series* **202**, 1–6.

Gneiting, T. and Schlather, M. (2004). Stochastic models that separate fractal dimension and the Hurst effect. *SIAM Review* **46**, 269–282. MR2114455 https://doi.org/10.1137/S0036144501394387

Goldberger, A. L., Amaral, L. A. N., Glass, L., Hausdorff, J., Ivanov, P. C., Mark, R. G., Mietus, J. E., Moody, G., Peng, C.-K. and Stanley, H. E. (2000). PhysioBank, PhysioToolkit, and PhysioNet: Components of a new research resource for complex physiological signals. *Circulation* **101**, e215–e220.

Hayes, B. (2003). The spectrum of Riemannium. *American Scientist* **91**, 296–300.

Jørgensen, B. (1997). *The Theory of Dispersion Models*. London: Chapman & Hall. MR1462891

Jørgensen, B. and Kokonendji, C. C. (2011). Dispersion models for geometric sums. *Brazilian Journal of Probability and Statistics* **25**, 263–293. MR2832887 https://doi.org/10.1214/10-BJPS136

Jørgensen, B., Martínez, J. R. and Tsao, M. (1994). Asymptotic behaviour of the variance function. *Scandinavian Journal of Statistics* **213**, 223–243. MR1292637

Kantelhardt, J., Koscielny-Bunde, E., Rego, H., Havlin, S. and Bunde, A. (2001). Detecting long-range correlations with detrended fluctuation analysis. *Physica A* **295**, 441–454.

Keeling, M. and Grenfell, B. (1999). Stochastic dynamics and a power law for measles variability. *Philosophical Transactions of the Royal Society of London Series B, Biological Sciences* **354**, 769–776.

Kendal, W. (2017). $1/f$ noise and multifractality from bristlecone pine growth explained by the statistical convergence of random data. *Proceedings—Royal Society Mathematical, Physical and Engineering Sciences* **473**, 20160586. MR3621489 https://doi.org/10.1098/rspa.2016.0586

Kendal, W. S. (2001). A stochastic model for the self-similar heterogeneity of regional organ blood flow. *Proceedings of the National Academy of Sciences of the United States of America* **98**, 837–841. MR1814761 https://doi.org/10.1073/pnas.021347898

Kendal, W. S. (2014). Multifractality attributed to dual central limit-like convergence effects. *Physica A* **401**, 22–33. MR3294810 https://doi.org/10.1016/j.physa.2014.11.035

Kendal, W. S. (2015). Self-organized criticality attributed to a central limit-like convergence effect. *Physica A* **421**, 141–150. MR3294810 https://doi.org/10.1016/j.physa.2014.11.035

Kendal, W. S. and Jørgensen, B. (2011). Tweedie convergence: A mathematical basis for Taylor's power law, $1/f$ noise and multifractality. *Physical Review E* **84**, 066120.

Kendal, W. S. and Jørgensen, B. (2015). A scale invariant distribution of the prime numbers. *Computation* **3**, 528–540.

Kozubowski, T. J. and Podgórski, K. (2001). Asymmetric Laplace laws and modeling financial data. *Mathematical and Computer Modelling* **34**, 1003–1021. MR1858834 https://doi.org/10.1016/S0895-7177(01)00114-5

Leland, W. E., Taqqu, M. S., Willinger, W. and Wilson, D. V. (1994). On the self-similar nature of ethernet traffic. *IEEE/ACM Transactions on Networking* **2**, 1–15.

Mandelbrot, B. B. and van Ness, J. W. (1968). Fractional Brownian motions, fractional noises and applications. *SIAM Review* **10**, 422–437. MR0242239 https://doi.org/10.1137/1010093

McQuarrie, D. A. (1976). *Statistical Mechanics*. New York: Harper & Row.

Musha, T. and Yamamoto, M. (1997). $1/f$ fluctuations in biological systems. In *Proceedings—19th International Conference—IEEE/EMBS*, 2692–2697. *Chicago, IL*.

Muzy, J. F., Bacry, E. and Arnedo, A. (1993a). Multifractal formalism for fractal signals: The structure-function approach versus the wavelet-transform modulus-maxima method. *Physical Review E* **47**, 875–884.

Muzy, J. F., Bacry, E. and Arnedo, A. (1993b). Multifractal formalism for fractal signals: The struture-function approach versus the wavelet-transform modulus-maxima method. *Physical Review E. Statistical, Nonlinear, and Soft Matter Physics* **47**, 875–884.

Nurujjaman, M. and Sekar Iyengar, A. (2007). Realization of SOC behavior in a dc glow discharge plasma. *Physics Letters A* **360**, 717–721.

Pathria, R. K. (1972). *Statistical Mechanics*. Oxford: Pegamon Press.

Petterle, R. R., Bonat, W. H., Kokonendji, C. C., Seganfredo, J. C., Morares, A. and Gomes da Silva, M. M. (2019). Double Poisson–Tweedie regression models. *The International Journal of Biostatistics* **15**, 20180119. MR3962660 https://doi.org/10.1515/ijb-2018-0119

Philippe, P. (1999). The scale-invariant spatial clustering of leukemia in San Francisco. *Journal of Theoretical Biology* **199**, 371–381.

Press, W. (1978). Flicker noises in astronomy and elsewhere. *Comments on Astrophysics* **7**, 103–119.

Shan, C.-J., Cheng, W.-W., Liu, J.-B., Cheng, Y.-S. and Liu, T.-K. (2014). Scaling of geometric quantum discord close to a topological phase transition. *Scientific Reports* **4**, 1–6.

Stanley, H. E. and Meakin, P. (1988). Multifractal phenomena in physics and chemistry. *Nature* **335**, 405–409.
Susskind, L. and Hrabovsky, G. (2013). *The Theoretical Minimum*. New York: Basic Books.
Szendro, P., Vincze, G. and Szasz, A. (2001). Pink-noise behaviour of biosystems. *European Biophysics Journal* **30**, 227–231.
Takahashi, K. (1989). Detection of solar neutrons by ground-based neutron monitor. *Space Science Reviews* **51**, 123–146.
Taylor, L. R., Taylor, R. A. J., Woiwod, I. P. and Perry, J. N. (1983). Behavioural dynamics. *Nature* **303**, 801–804.
Tsybakov, B. and Georganas, N. D. (1997). On self-similar traffic in ATM queues: Definitions, overflow probability bound, and cell delay distribution. *IEEE/ACM Transactions on Networking* **5**, 397–409. MR1664070 https://doi.org/10.1109/18.705538
Tweedie, M. C. K. (1984). An index which distinguishes between some important exponential families. In *Statistics: Applications and New Directions* (J. K. Ghosh and J. Roy, eds.). *Proceedings of the Indian Statistical Institute Golden Jubilee International Conference*, 579–604. Calcutta, India: Indian Statistical Institute. MR0786162
Usoskin, I., Kovaltsov, G., Kananen, H. and Tanskanen, P. (1997). The world neutron monitor network as a tool for the study of solar neutrons. *Annales Geophysicae* **15**, 375–386.
Vespignani, A. and Zapperi, S. (1998). How self-organized criticality works: A unified mean-field picture. *Physical Review E* **57**, 6345–6362. MR1628210 https://doi.org/10.1103/PhysRevE.57.6345
Werndl, C. (2009). What are the new implications of chaos for unpredictability? *British Journal for the Philosophy of Science* **60**, 195–220. MR2485508 https://doi.org/10.1093/bjps/axn053
Wigner, E. P. (1967). Random matrices in physics. *SIAM Review* **9**, 1–23.

Department of Physics
University of Ottawa
Ottawa
Canada
E-mail: wkend037@uottawa.ca